Heat Transfer and Fluid Flow through Microchannels – a theoretical approach

N.AMANIFARD, M.BORJI, A.K. HAGHI *
Faculty of Engineering
The University of Guilan
P.O. Box 3756, Rasht
IRAN
http://www.guilan.ac.ir

Abstract: Three dimensional heat transfer and water flow characteristic in a set of rectangular microchannel heat sinks for advanced electronic systems investigated in this paper. The full Navier-Stoke's approach is employed for this kind of narrow channels for the water flow assessments. The complete form of the energy equation accompanying the dissipation terms is also linked to the momentum equations. The calculated thermal distribution show good agreements with the corresponding experimental predictions. Then these results are compared with porous medium approach in small dimensions. In this approach microchannel is modeled as a fluid-saturated porous medium, and is numerically solved based on the Forchheimer-Brinkman-extended Darcy equation for the fluid flow and two equation model for heat transfer between the solid and fluid phase.

Key-Words: Porous medium- Microchannel heat sink- Heat transfer- Velocity profile.

1 Introduction

The increasing incorporation of electronic systems requires innovative, small scale and highly effective cooling techniques for the removal of a large amount of heat from a small area in order to avoid its temperature from rising significantly and operate electronic devise at an optimum temperature. Many techniques have been developed for controlling and removing the heat generated in such a case. One such method is to use microchannel heat sinks. Microchannel heat sink is a structure with many micro scale channels of large aspect ratio built on the back of the microchip, and a liquid is forced through these passages to carry out the energy. The microchannel heat sink at first proposed by Tuckermann and Pease [1], they demonstrated that the microchannel heat sinks, consisting of micro-rectangular flow passages, have a higher heat transfer coefficient in laminar flow regime than that in turbulent flow through conventionally-sized devices. Since pioneering work of Tuckerman and Pease [1], many experimental, analytical and numerical investigations are reported. Peng and Wang [2] and Peng and Peterson [3] systematically examined the forced flow and heat transfer characteristics of water and binary mixtures flowing through rectangular microchannels. It was observed that laminar flow transition occurred at Reynolds number between 200 and 700. And the critical transition Reynolds number diminished with the decrease in the size of the microchannel. Furthermore, the effects of aspect ratio and the hydraulic diameter on the flow and heat transfer in microchannel were investigated. These results provided noticeable experimental data and considerable manifestation that the flow and heat transfer in microchannels are strongly dependent upon the type and properties of the working fluid as well as geometric parameters of microchannels [4], and therefore may be different from what typically occur in the macrochannels. Wilding et al [5] analyzed flow of water and various biological fluids in glass-capped silicon microchannels. The data illustrated an approximately 50% increase in the Darcy friction factor from the theoretical results. Similar results were observed by Jiang et al [6] who studied flow of water through rectangular and trapezoid cross-section channels. The microchannels used in this study were formed by etching a silicon substrate and capping it with a glass wafer. Alternatively, in view of the small dimensions of the microstructures, Koh and Colony [7] modeled the microchannels as a porous medium by using Darcy's law to describe the flow. Later, Kim and Kim [8] and Kim et al. [9] have presented analytical solutions for velocity and temperature distributions for forced convection in microchannel heat sinks by using the Brinkman-extended Darcy equation for the

fluid flow. More recently Amanifard et al. [10] numerically investigated the effect of electrical double layer (EDL) near the solid/liquid interface, on three dimensional heat transfer characteristic and pressure drop of water flow through a rectangular microchannel. The results illustrate that, the liquid flow in rectangular microchannels is influenced significantly by the EDL, particularly in the high electric potentials, and hence deviates from flow characteristics described by classical fluid mechanics.

In this paper the compatibility and effectiveness of Navier-Stokes and energy correlation in microscale channels is numerically verified based on the experimental results of Tuckerman and Pease [1].

2 Physical model and computational domain

A schematic view, physical, and computational domain of such microchannels is depicted in Fig (1), Fig (2), and Fig (3), respectively. Heat is removed primarily by conduction through the solid and then dissipated away by convection of the cooling fluid in the microchannel. The microchannel has been studied is made of silicon with thermal conductivity (k) of $148 W/m.K$. At the bottom, a uniform heat flux of q" arises from an electric chip that is connected to the microchannel. At the top of the channels, there is a Pyrex plate which makes an adiabatic condition. The width of microchannels and the wall thickness are represented by W_c and W_s, respectively. The thickness of the silicon substrate through which the heat flux is transformed to the cooling fluid flowing in channels can be simply recognized as H_t-H_c, according to Fig (1). The total length and width of microchannels are L_h and W_t whose values of five different cases are in Table (1). Moreover, steady incompressible and laminar fluid flow and steady heat transfer, with negligible radiative heat transfer and constant solid and fluid property have been assumed in computations. The inlet temperature of cooling water through the channels is 20ºC. A microchannel in the center parts of the plate will be considered in current work. As a result of the symmetry of the rectangular channel, we will center the computational domain in a half channel as shown in Fig (3).

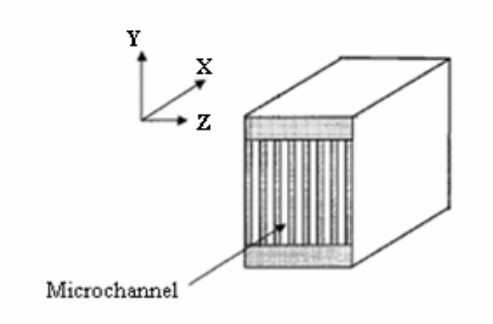

Figure (1) Schematic of microchannel

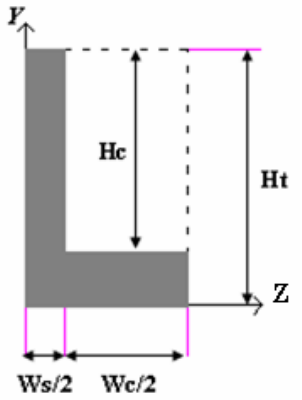

Figure (2) physical model

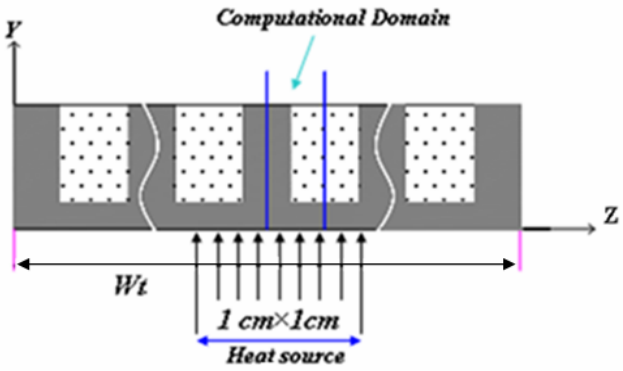

Figure (3) Computational domain

Table (1) Five different cases of microchannels

Descriptions	$W_c(\mu m)$	$H_c(\mu m)$	$L_t(cm)$	q"(W/cm^2)	Inlet Velocity (m/s)	Aspect ratio	Nusselt number
Case 1	64	280	2	34/6	0/7	4.375	7.01
Case 2	56	320	1/4	181	1/3	5.71	13.627
Case 3	55	287	1/4	277	2	5.218	15.155
Case 4	50	302	1/4	790	2/85	6.04	16.54

3 Governing Equations

Assuming a laminar fully developed flow in rectangular channels in positive x-direction, the components of velocity satisfy $u = u(y,z)$ and $v = w = 0$ in terms of Cartesian coordinate system. The equation of motion is written as follows:

$$\frac{\partial^2 u}{\partial y^2} + \frac{\partial^2 u}{\partial z^2} = \frac{1}{\mu_f}\frac{dP}{dx} \tag{1}$$

As presented in Fig (1), a silicon wafer plate with a large number of microchannels is connected to the chip. A liquid is forced to flow through these microchannels to remove the heat. All microchannels are assumed to have a uniform rectangular cross-section with geometric parameters as shown in Table 1. For a steady-state, fully developed, laminar flow in a microchannel, the energy equation (with consideration of the axial thermal conduction in flow direction and the viscous dissipation) for the cooling liquid takes the specific form:

$$u\frac{\partial T}{\partial x} = \alpha_f\left(\frac{\partial^2 T}{\partial x^2} + \frac{\partial^2 T}{\partial y^2} + \frac{\partial^2 T}{\partial z^2}\right) + \frac{\mu_f}{\rho_f C_{pf}}\left[\left(\frac{\partial u}{\partial y}\right)^2 + \left(\frac{\partial u}{\partial z}\right)^2\right] \tag{2}$$

Where T and α_f are the temperature and the thermal diffusivity of the cooling liquid, respectively, C_{pf} is the specified heat capacity of the cooling liquid. Based on presented computational domain, the adiabatic condition can be used along the channel symmetric center line:

$$z = 0 \quad \Rightarrow \quad \frac{\partial T}{\partial z} = 0 \tag{3}$$

At the bottom of channels, a uniform heat flux of q" is imposed over the heat sink, and can be expressed as:

$$y = 0 \quad \Rightarrow \quad q'' = -k_f\left(\frac{\partial T}{\partial y}\right) \tag{4}$$

Hear k_f is the thermal conductivity of the liquid coolant. Since the thermal conductivity of the glass is about two-order of magnitude lower than that the top boundary is insulted. This is a conservative assumption which will lead to slight underestimation of the overall heat transfer coefficient. This assumption yields:

$$y = H_c \quad \Rightarrow \quad \frac{\partial T}{\partial y} = 0 \tag{5}$$

4 Numerical solution method

In current work finite volume method of Patankar [13] is used to solve the continuity, momentum, and energy equations numerically. Since a detailed discussion of the FVM is available in Patankar [13], only a very brief description of the main features of this method is given here.

In the FVM, the domain is divided into a number of control volumes such that there is one control volume surrounding each grid point. The grid point is located in the center of a control volume. The governing equation is integrated over each control volume to derive an algebraic equation containing the grid point values of the dependent variable. The discretization equation then expresses the conservation principle for a finite control volume just as the partial differential equation expresses it for an infinitesimal control volume. The resulting solution implied that the integral conservation of quantities such as mass, momentum, and energy is exactly satisfied for any control volume and of course, for the whole domain. The power-low scheme is used to model the combined convection-

diffusion effects in the transport equations. The SIMPLER algebraic of Patankar is used to resolve the pressure-velocity coupling. The resulting algebraic equations are solved using a line-by-line Tri-Diagonal matrix Algorithm.

5 Microchannel as a porous medium

In view of the small dimensions of the microstructures, the microchannel is modeled as a fluid-saturated porous medium. By following a procedure described by Chien-Hsin Chen [11] the flow is assumed to be laminar and both hydrodynamically and thermally fully developed. Also, the thermal physical properties are assumed to be constant. To relax the constant-fluid temperature assumption along the height of the channel wall, the microchannel heat sinks is modeled as a fluid-saturated porous medium, as shown in Fig (4). The Forchheimer-Brinkman-extended Darcy equation proposed by Vafai and Tien [12] for the fluid flow and the volume-averaged two-equation model for heat transfer are used. The summary of equations and boundary conditions by using following non-dimensional groups can be expressed in dimensionless form as follows, and complete equations can be observed in Chen's work [11];

$$Y=\frac{y}{H_c},\ U=\frac{\langle u_f\rangle}{u_D},\ \theta_f=\frac{\langle T\rangle_f-T_w}{q_w H_c/(1-\varepsilon)k_s},\ \theta_s=\frac{\langle T\rangle_s-T_w}{q_w H_c/(1-\varepsilon)k_s} \tag{6}$$

Where the bracket $\langle\ \rangle$ represents a volume-averaged value, and ε, k_s, and $u_D=-\frac{K}{\varepsilon\mu_f}\frac{d\langle p\rangle_f}{dx}$ are porosity, thermal conductivity of solid and Dacian convective velocity, respectively.

$$\frac{Da}{\varepsilon}\frac{d^2U}{dY^2}-\Gamma U^2-U+1=0 \tag{7}$$

$$\frac{d^2\theta_s}{dY^2}-\widetilde{Bi}(\theta_s-\theta_f)=0 \tag{8}$$

$$k_r\frac{d^2\theta_f}{dY^2}-\widetilde{Bi}(\theta_s-\theta_f)-SU=0 \tag{9}$$

$$U=0 \quad at \quad Y=0,1 \tag{10}$$

$$\theta_s=\theta_f=0 \quad at \quad Y=0 \tag{11}$$

$$\frac{\partial\theta_s}{\partial Y}=\frac{\partial\theta_f}{\partial Y}=0 \quad at \quad y=1 \tag{12}$$

Where

$$Da=\frac{K}{H_c^2},\quad \Gamma=\frac{\rho_f u_D CK}{\varepsilon\mu_f} \tag{13}$$

Are the Darcy number and the inertial force parameter, respectively. And S is given by

$$S=\frac{1}{\int_0^1 UdY} \tag{14}$$

The parameters K_r and $\widetilde{Bi}$ are the effective thermal conductivity ratio and the equivalent Biot number in porous medium model, respectively, and can be written as

$$k_r=\frac{k_{fe}}{k_{se}}=\frac{\varepsilon k_f}{(1-\varepsilon)k_s},\qquad \widetilde{Bi}=\frac{haH^2}{k_{se}}=10k_r\alpha_s^2 \tag{15}$$

Where K, C, k_{sc}, h, a, and k_{fc} are the permeability, inertial force coefficient, effective thermal conductivity of solid, interstitial heat coefficient, wetted area per volume, and effective thermal conductivity of the fluid, respectively. The porosity, the wetted area per volume, and effective thermal conductivities can be expressed as

$$\varepsilon=\frac{w_c}{w_c+t}\quad,\quad a=\frac{2}{w_c+t} \tag{16}$$

$$k_{se}=(1-\varepsilon)k_s\qquad,\qquad k_{fe}=\varepsilon k_f \tag{17}$$

And k_f is the thermal conductivity of fluid. Permeability and the interstitial heat transfer coefficient can be written as

$$K=\frac{\varepsilon\mu_f}{-(dp/dx)}\langle u\rangle_f=\frac{\varepsilon w_c^2}{12} \tag{18}$$

$$h=\frac{q''}{T_w-\langle T\rangle_f}=\frac{5k_f}{w_c} \tag{19}$$

The energy carried by the fluid as it moves past a given cross section is

$$\dot{m}c_f\langle T\rangle_{f,m}=\int_{A_c}\rho_f c_f\langle T\rangle_f\langle u\rangle_f dA \tag{20}$$

Here $\dot{m}$ is the mass flow rate and $\langle T\rangle_{f,m}$ is the bulk mean fluid temperature using volume-averaged values. For constant-fluid properties,

$$\langle T\rangle_{f,m}=\frac{1}{u_m A_c}\int_{A_c}\langle u\rangle_f\langle T\rangle_f dA \tag{21}$$

$$\overline{Nu}=\frac{\bar{h}H_c}{k_f} \tag{22}$$

$$\bar{h}=\frac{q_w}{T_w-T_{f,m}} \tag{23}$$

Where $T_{f,m}$ is the conventional bulk mean temperature and can be written as

$$T_{f,m} = \frac{1}{u_m A_c} \int_{A_c} u_f T_f dA \tag{24}$$

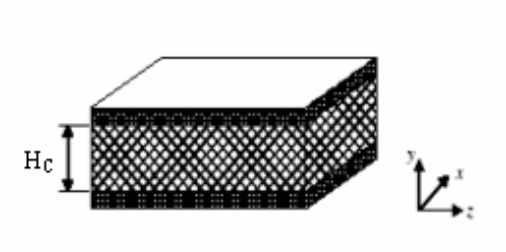

Figure (4) the equivalent porous medium

6 Results and discussions

For solving the equations several grid structures were used. The grid density of 120×40×20 in *z*, *y*, and *x* directions is considered to be appropriate. Thermal resistance can be simply computed using

$$R(z) = \frac{T_{\max}(z) - T_{\text{in}}}{q} \tag{25}$$

In equation (25), T_{out} and T_{in} represent the measured outlet and inlet temperature of cooling water, respectively, and q is the heat flux. The computed thermal resistances in four different cases are compared with those of experimental results conducted by Tuckerman and Pease [1] in table (2). It is shown that sufficiently reasonable agreement exists in such comparison and, therefore, full Navier-Stokes approach can be deployed for such microchannels flow and heat transfer computation with a hydraulic diameter of about 100 μm. The Nusselt number (Nu) are computed as

$$Nu = \frac{hD_h}{K_f} \tag{26}$$

And hydraulic diameter D_h is defined as follows

$$D_h = \frac{2H_c W_c}{H_c + W_c} \tag{27}$$

We can see in case 4 with 790 w/cm^2 heat flux, only 67.94℃ increasing in cooling water temperature.

Fig (5) illustrates the velocity profiles in various *y-z* sections in Case 1. As it can be seen, the velocity gradient near the channel walls is very large. This large velocity gradient shows that the wall shear stress is considerably large; so the pressure drop along the channel will be significant. Although the thermal boundary layer of flow through channel is fully developed, the assumption of fully developed velocity boundary layer is wrong. Fig. 5 shows that the velocity profile through whole channel is not developed and the entry region effects are noticeable. The main reason of pressure drop in these cases is the developing velocity profile which increases the wall shear stress. These results are not consistent with Tuckerman's experiments. So there must be some modifications in the governing equations to reach the accurate results.

Table (2) Thermal resistance comparison

Case	$q(\frac{W}{cm^2})$	$R(cm^2K/W)$		Error (%)
		Experimental	Numerical	
0	34.6	0.277	0.253	8.5
1	34.6	0.28	0.246	12.1
2	181	0.110	0.116	5
3	277	0.113	0.101	8.1
4	790	0.090	0.086	3.94

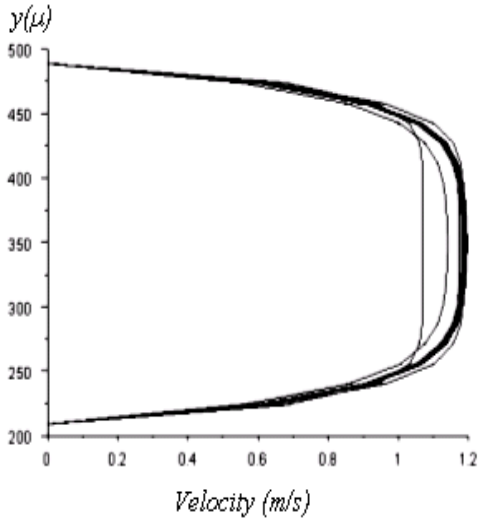

Figure (5) Velocity profiles in *y-z* sections for Case 1

In Fig (6), we can see the dimensionless velocity profile for various values of aspect ratio and inertial force parameter in porous medium approach. As illustrated in this Figure, the velocity profile shows a reasonable agreement in two methods at aspect ratios about 3 to 6. But the deviation of two methods appears with increasing the inertial force parameter (Γ) and decreasing the aspect ratio.

The effect of various problem parameters on the Nusselt number is illustrated in Figs (7) and (8). It is clear from this figures and table 1 that the Nusselt number increases with increasing the aspect ratio in two methods. As depicted in Fig (7), for a given

aspect ratio, a larger porosity will produce a larger Nusselt number. Fig (7) unveils that the variation of inertial force parameter can only results a slight similar variation in Nusselt number. It's evident that for a specified aspect ratio, conform of two methods is disrupted with increasing the porosity. But in small porosities two solutions show a good accommodation.

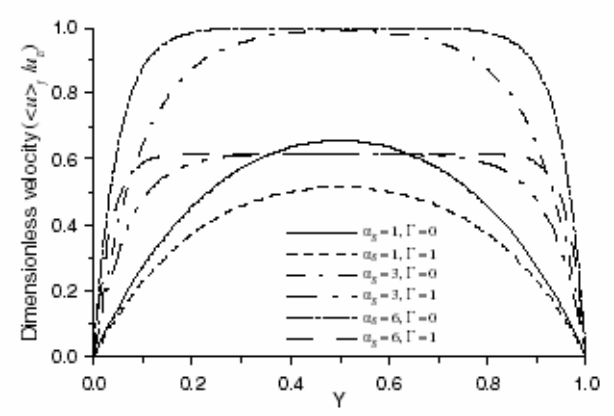

Figure (6) Dimensionless velocity profiles for various values of α_s and Γ

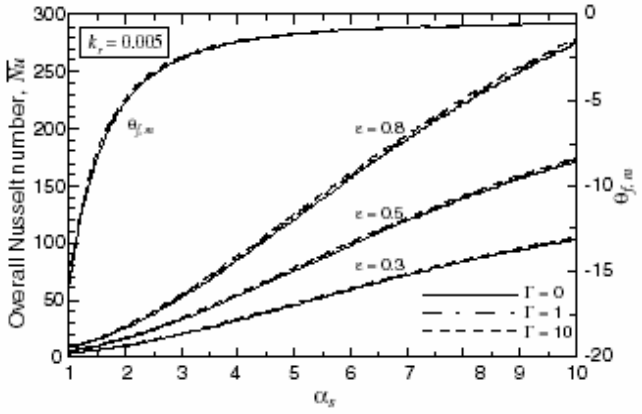

Figure (7) Overall Nusselt number vs. α_s at selected values of ε and Γ

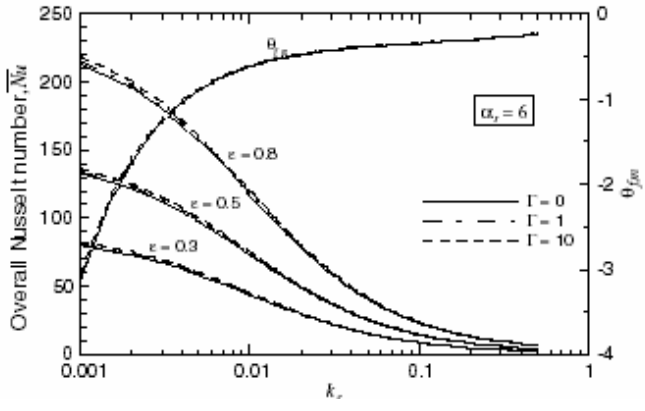

Figure (8) Overall Nusselt number vs. k_r at selected values of ε and Γ

7 Conclusion

In this work the heat transfer in four geometric types of microchannel heat sinks has been investigated. The numerical results are obtained for thermal resistance and the Nusselt number and show a good agreement with experimental data. The Nusselt number is found to increase with increasing the aspect ratio. The results also gave the required assurance of using the full Navier-Stokes approach for the microchannels with hydraulic diameters about 100 μm. The velocity profile shows an entry length area in the channel and therefore, a high gradient temperature and velocity profiles were achieved. In addition, based on the Chen's work et. al. [11], the effect of various parameters as; channel aspect ratio, inertial force parameter, and the porosity on the Nusselt number and velocity profile in porous medium approach are investigated. The comparison between two methods showed a good agreement at aspect ratios about 3 to 6 for velocity profile and in small porosities for Nusselt number.

References:

[1] D.B. Tuckermann, and R.F.W. Pease, High-performance Heat Sinking for VLSI, IEEE Electron. Dev.Lett.EDL-2, pp. 126-129 (1981).

[2] X.F. Peng, G.P. Peterson, and Wang, B.X., Heat transfer characteristics of water flowing through microchannels. Experimental Heat transfer 7,pp 265-283 (1994).

[3] Peng, X.F., and Peterson, G.P., Forced convection Heat Transfer of single-phase binary mixture through microchannels. Experimental Thermal and fluid science 12 pp 98-104(1996).

[4] B.X. Wang, X.F. Peng, Experimental Investigation on liquid forced convection heat transfer through microchannels, International Journal of Heat and Mass Transfer 37 (supple.1), pp 73-82(1994).

[5] P. Wilding M. A. Shoffner, and L. J. Kircka., Manipulation and Flow of Biological Fluids in Straight channels micromachined in Silicon, Clin. Chem., vol. 40, pp. 43-47, (1994).

[6] X. N. Jiang, Z.Y. Zhou, J. Yao, Y. Li, and X. Y. Ye, Micro-fluid Flow in Microchannel, In proc. Transdueers 95, Stockholm, Sweden, June 25-29, pp. 317-320, (1995).

[7] J.C.Y. Koh, R. Colony, Heat transfer of microstructures for integrated circuits, Int. Commun. Heat Mass Transfer 13 (1986) 898-98.

[8] S.J. Kim, D. Kim, Forced convection in

microstructures for electronic equipment cooling, ASME J. Heat Transfer 121 (1999) 635-645.
[9] S.J. Kim, D. Kim, D. Y. Lee, on the local thermal equilibrium in microchannel heat sinks, Int. J. Heat Mass Transfer 43 (2000) 1735-1748.
[10] N. Amanifard, M. Borji, A. K. Haghi, Heat Transfer in porous medium, Brazilian J. Chemical engineering 24 (2007)-in press.
[11] Chien-Hsin Chen, forced convection heat transfer in microchannel heat sinks, Int. J. Heat and Mass Transfer 50 (2007)2182-2189.
[12] K. Vafai, C.L Tien, Boundary and inertia effects on flow and heat transfer in porous media, Int, J, Heat Mass Transfer 24(1981) 195-203.
[13] S.V.Patankar, Numerical Heat Transfer and Fluid Flow, Hemisphere, New York, 1980.